

ChemComm

Accepted Manuscript



This is an *Accepted Manuscript*, which has been through the Royal Society of Chemistry peer review process and has been accepted for publication.

Accepted Manuscripts are published online shortly after acceptance, before technical editing, formatting and proof reading. Using this free service, authors can make their results available to the community, in citable form, before we publish the edited article. We will replace this *Accepted Manuscript* with the edited and formatted *Advance Article* as soon as it is available.

You can find more information about *Accepted Manuscripts* in the [Information for Authors](#).

Please note that technical editing may introduce minor changes to the text and/or graphics, which may alter content. The journal's standard [Terms & Conditions](#) and the [Ethical guidelines](#) still apply. In no event shall the Royal Society of Chemistry be held responsible for any errors or omissions in this *Accepted Manuscript* or any consequences arising from the use of any information it contains.

COMMUNICATION

“Converting” an hexametallc Mn^{III} wheel to a dodecametallic Mn^{III} wheel *via* ligand oximation

Cite this: DOI: 10.1039/x0xx00000x

Sergio Sanz,^a Jamie M. Frost,^a Mateusz B. Pitak,^b Simon J. Coles,^b Stergios Piligkos,^c Paul J. Lusby^a and Euan K. Brechin^{*a}Received 00th January 2012,
Accepted 00th January 2012

DOI: 10.1039/x0xx00000x

www.rsc.org/

Ligand oximation “converts” an hexametallc Mn^{III} wheel into a dodecametallic Mn^{III} wheel, while the magnetic exchange switches from ferro- to antiferromagnetic.

Understanding the fundamentally important relationship between molecular structure and magnetic behaviour requires the construction of large families of related molecules.¹ Ligand design is therefore a vital component for the construction of polymetallic molecules, and scientists interested in investigating the magnetic properties of cages containing multiple paramagnetic metal ions have employed synthetic strategies encompassing the whole spectrum from “predictable” to “serendipitous” self-assembly employing both rigid and flexible structural building blocks.² Indeed hundreds if not thousands of beautiful cluster compounds with fascinating physical properties have been reported for more than half a century.³ Mining structural databases provides invaluable information about what synthetic strategies have been most successful, and perhaps more importantly informs us of the ligand bridging moieties that are most prominent for a particular metal in a particular oxidation state. For Mn^{III} a search of the CSD reveals that phenolic oximes⁴ and diols⁵ are two particularly successful examples. The former are somewhat more rigid and predictable in their behaviour, commonly μ -bridging, while the latter are more flexible (μ - to μ_5 -bridging) and thus rather unpredictable, although each alkoxide moiety within the ligand is more often than not found to be μ -bridging. Herein we introduce two new ligand systems, H₃L¹ and H₄L² (Figure 1), for the synthesis of Mn^{III} wheels. The latter is analogous to the former but with the ketone moiety oximated. This simple change converts it from a tridentate to a tetradentate ligand and the result is a doubling in the size of the wheel.

Reaction of MnCl₂·4H₂O and H₃L¹ in a basic MeOH solution produces hexagonal black crystals of [Mn^{III}₆Na(L¹)₆]Cl (**1**) after five days (see the ESI for full details). The crystals were in a

cubic crystal system and structure solution was obtained in the *Ia-3d* space group†. The structure (Figure 2) describes a Na⁺-centred [Mn^{III}₆] wheel in which all the Mn^{III} ions and ligands are symmetry equivalent. The ligand is fully deprotonated and μ_3 -bridging: the N-atom and phenolic O-atom are terminally bonded with one alkoxide arm (O3) bridging between neighbouring Mn^{III} ions (Mn-O3-Mn, 110.25°), the other (O4, Mn-O4-Mn, 101.29°) doing likewise, but also bridging to the central Na⁺ ion. The ketone moiety remains non-bonded. The Mn^{III} ions are all six coordinate in distorted octahedral geometries, their Jahn-Teller axes being defined by the N1-Mn1-O4 vector. The distance between neighbouring Mn^{III} ions is 3.25 Å and the radius of the wheel (Mn...Mn) is ~6.5 Å. The central Na⁺ is restrained by symmetry to be six coordinate and octahedral with Na-O4 = 2.314 Å. In the crystal the molecules pack in an aesthetically pleasing manner (Figure S1), with large accessible voids containing the Cl⁻ counter ions and heavily disordered solvent molecules. The closest cation...anion distances are of the order ~3.5 Å to the C atoms of the diol and ketone moieties, with the closest cluster...cluster interactions approximately 3.6 Å (C(Ph)...C(Ph); O(ketone)...C(diols)).

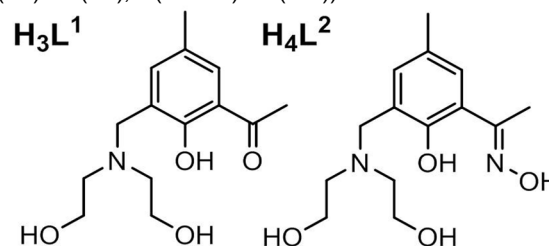


Figure 1. The structures of H₃L¹ (left) and H₄L² (right).

A similar reaction but employing H₄L² produces the dodecametallic complex [Mn^{III}₁₂(OMe)₂₀(L²)₄] (**2**) as brown plates in the monoclinic space group *P2₁/n*. The structure (Figure 3)

contains a non-planar, saddle-shaped dodecametallic wheel. The Mn^{III} ions are all symmetry inequivalent, but there is repetition in the pattern of ligand bridging (Figure 3C): the first two Mn^{III} ions are bridged by two μ -methoxides, the next two Mn^{III} ions are bridged by one μ -methoxide and one μ -alkoxide of the diethanolamine moiety, and the third pair of Mn^{III} ions is bridged by two μ -methoxides and the –N–O– moiety of the phenolic oxime unit. The phenolic O-atom is terminally bonded (~ 1.89 Å), as is the remaining O-atom (~ 1.92 Å) of the diol moiety; the fully deprotonated L² ligand is thus μ_4 -bridging. The Mn–O(OMe)–Mn bridging angles are rather varied, ranging from 91.95–104.99°; while the Mn–O(diol)–Mn angles all fall in the 103.78–105.39° range. The Mn–O–N–Mn torsion angles are all rather small, 6.77–16.78°. The Mn^{III} ions are all six coordinate and in distorted octahedral geometries, with the positions of the Jahn-Teller axes depicted in Figure 3D. The wheel is approximately 10 Å in diameter. The closest inter-cluster contacts are of the order of 3.4 Å between the methyl group of the phenyl rings to the phenoxide O-atoms and the –CH₂ groups of the diol moiety (Figure S2).

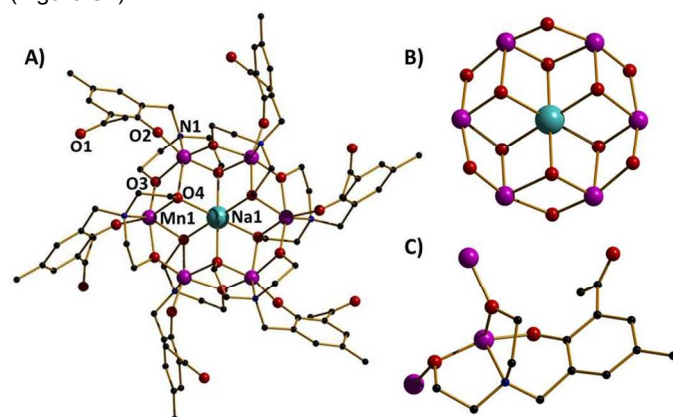


Figure 2. (A) The structure of the cation of **1**, viewed perpendicular to the [Mn^{III}₆] plane. (B) The magnetic core. (C) The bridging mode of the ligand. Colour code: Mn = purple, Na = light blue, O = red, N = dark blue, C = black. H atoms and Cl[–] anions omitted for clarity.

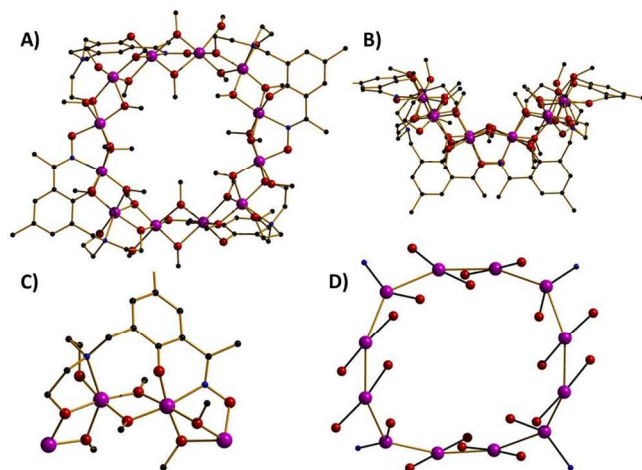


Figure 3. The structure of complex **2**, viewed (A) perpendicular and (B) parallel to the [Mn^{III}₁₂] “plane”. H atoms and Cl[–] anions omitted for clarity. (C) The “repeat”

unit of the wheel highlighting the ligand bridging modes. (D) Metallic skeleton highlighting the Jahn-Teller axes. Colour code: Mn = purple, O = red, N = blue, C = black. H-atoms omitted for clarity.

A search of the CSD reveals there to be eleven examples of [Mn^{III}₆] wheels, of which five are centred wheels containing an alkali metal cation; three of these contain Na, two Ce and one Li.⁶ [Mn₁₂] wheels are far more unusual, indeed there are only three reported in the literature and only one of those, the complex [Mn₁₂(tpeshz)₁₂(dmf)₁₂] (H₃tpeshz = *N-trans*-2-pentenoylsalicylhydrazide), contains Mn exclusively in the III+ oxidation state.⁷

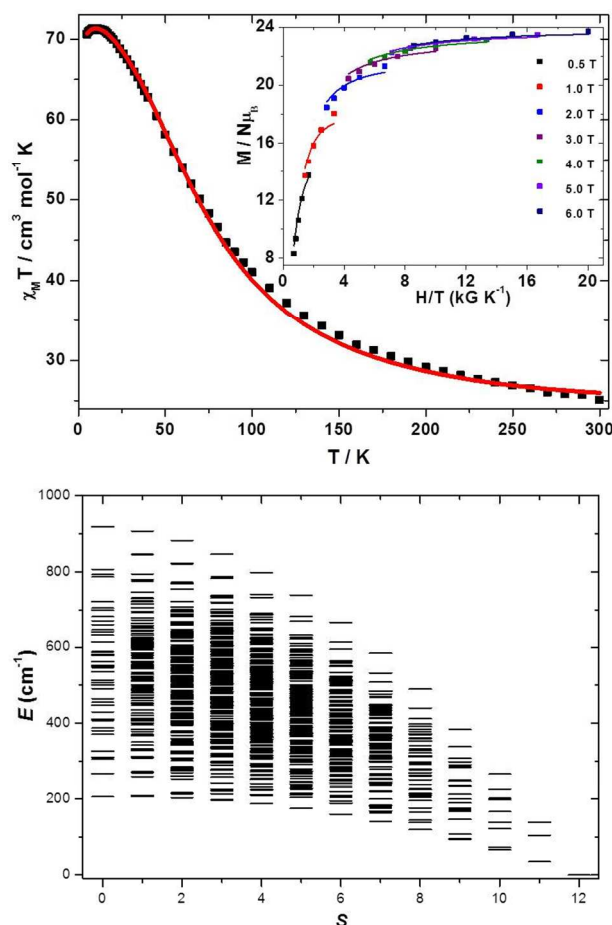


Figure 4. (top) Plot of the $\chi_M T$ product versus T for **1**. The inset shows a plot of reduced magnetisation. Solid lines are a fit of the experimental data. See text for details. (bottom) Plot of energy versus total spin state, derived from the isotropic fit of the susceptibility.

Direct current magnetic susceptibility studies were performed on polycrystalline samples of **1** and **2** in the 5–300 K range in an applied field of 0.1 T. The results are plotted as the $\chi_M T$ product versus T in Figure 4 and Figure S3. For **1** the $\chi_M T$ value of ~ 26 cm³ K mol^{–1} at 300 K is above the spin-only ($g = 2.0$) value of 18 cm³ K mol^{–1} expected for six non-interacting high-spin Mn^{III} (3d⁴) ions. The value increases constantly with decreasing temperature reaching a maximum value of ~ 71 cm³ K mol^{–1} at 10 K, where it then plateaus. This behaviour is indicative of the presence of ferromagnetic exchange between neighbouring

metal ions. The experimental data can be fitted to the isotropic spin-Hamiltonian (1), by use of the Levenberg–Marquardt algorithm⁸:

$$\hat{H}_{iso} = -2 \sum_{i,j>i} J \hat{S}_i \cdot \hat{S}_j + \mu_B H g \sum_i \hat{S}_i \quad (1)$$

where i, j are indices running through the constituent single ions, J is the isotropic exchange parameter, \hat{S} is a spin operator, μ_B is the Bohr magneton, $g = 2.0$ is the g -factor of Mn^{III} and H is the applied magnetic field. We have used a "wheel" model, including just one exchange interaction between nearest neighbours. This affords $J = +8.64 \text{ cm}^{-1}$ with the resulting $S = 12$ ground state being separated by $\sim 35 \text{ cm}^{-1}$ from the first ($S = 11$) excited state (Figure 4, bottom). A ferromagnetic interaction for this molecule is expected based on a recently published magnetostructural correlation (MSC) for alkoxide-bridged Mn^{III} dimers in which ferromagnetic exchange is predicted when neighbouring Jahn-Teller axes are arranged perpendicular to each other.⁹ The magnitude of the exchange observed in **1** is also consistent with this MSC. Magnetisation data (Figure 4, top, inset) collected in the 2–7 K and 0.5 – 6.0 T temperature and field ranges can be fitted by assuming only the ground spin-state is thermally populated under these experimental conditions. We therefore used anisotropic spin-Hamiltonian (2) that takes into account spin-variables relevant to the $S = 12$ ground spin-state only,

$$\hat{H}_{aniso} = D_{S=12} \left[\hat{S}_z^2 - (S+1)S/3 \right] + \mu_B H g \sum_i \hat{S}_i \quad (2)$$

where D is the uniaxial anisotropy parameter of the $S = 12$ ground spin-state. Spin-Hamiltonian (2) was fitted to the experimental data by use of the simplex algorithm,⁸ to give the best-fit parameter $D_{(S=12)} = -0.086 \text{ cm}^{-1}$.

For complex **2**, the $\chi_M T$ value of $\sim 35 \text{ cm}^3 \text{ K mol}^{-1}$ at 300 K is slightly below the spin-only value of $36 \text{ cm}^3 \text{ K mol}^{-1}$ expected for twelve non-interacting high-spin Mn^{III} ions (Figure S3). The value decreases continually with decreasing temperature reaching a minimum value of $\sim 12.5 \text{ cm}^3 \text{ K mol}^{-1}$ at 5 K. This behaviour is indicative of the presence of antiferromagnetic exchange between neighbouring metal ions, and the presence of a small or diamagnetic spin ground state. This is corroborated by the magnetisation data (Figure S4) which rises in a near linear fashion with field and does not reach saturation. The sheer size of the cage precludes any quantitative analysis of the data. Neither complex shows any frequency-dependence in ac susceptibility above 2 K, ruling out slow relaxation of the magnetisation, at these temperatures.

At this stage it is difficult to determine the fundamental reasons why the magnetic exchange is ferromagnetic in **1**, but antiferromagnetic in **2**. From a structural perspective, the most obvious difference is the introduction of the bridging oxime -N-O- moiety in **2**. However, given the structural complexity of compound **2**, unravelling the answer will require both the construction of new family members and detailed theoretical analysis.

Conclusions

Combining phenolic oxime and diethanolamine fragments into the same organic framework affords the novel pro-ligands H_3L^1 and H_4L^2 and their initial use in Mn^{III} chemistry has led to the isolation of unusual hexa- and dodecametallic wheels; oximation of the ligand doubling the nuclearity of the wheel. The former complex displays dominant ferromagnetic exchange interactions and an $S = 12$ ground state, the latter antiferromagnetic exchange and a small or diamagnetic ground state. Given that this is the first investigation into the coordination chemistry of these two organic molecules, it is likely that many more polymetallic cages can be isolated. More generally, the concept of incorporating previously successful but independent ligands into one framework is likely widely applicable.

Notes and references

^aEaStCHEM School of Chemistry, The University of Edinburgh, West Mains Road, Edinburgh, EH9 3JJ, UK. Email: ebrechin@staffmail.ed.ac.uk

^bUK National Crystallography Service, Chemistry, Faculty of Natural and Environmental Sciences, University of Southampton, Highfield Campus, Southampton, SO17 1BJ, UK

^cDepartment of Chemistry, University of Copenhagen, Universitetsparken 5, DK-2100, Denmark.

†Crystal data for **1**: $C_{84}H_{108}ClMn_6N_6NaO_{24}$, $M = 1973.84$, cubic, space group $Ia\bar{3}d$, $a = 36.229(15) \text{ \AA}$, $\alpha = 90^\circ$, $V = 47552(59) \text{ \AA}^3$, $Z = 16$, $\mu = 0.639 \text{ mm}^{-1}$, $D_c = 1.103 \text{ Mg / m}^3$, 57326 reflections collected, 3502 unique ($R_{int} = 0.2067$), final $R_i = 0.1311$, $wR_2 = 0.3372$, $GoF = 1.226$, data/restraints/parameters = 3502/0/194. CCDC 977703.

Crystal data for **2**: $C_{80}H_{148}Mn_{12}N_8O_{40}$, $M = 2521.34$, monoclinic, space group $P2_1/n$, $a = 18.454(6)$, $b = 37.410(11)$, $c = 20.409(7) \text{ \AA}$, $\alpha = 90$, $\beta = 114.966(4)$, $\gamma = 90^\circ$, $V = 12773(7) \text{ \AA}^3$, $Z = 4$, $\mu = 1.212 \text{ mm}^{-1}$, $D_c = 1.311 \text{ Mg / m}^3$, 127080 reflections collected, 22227 unique ($R_{int} = 0.1745$), final $R_i = 0.0685$, $wR_2 = 0.1637$, $GoF = 1.009$, data/restraints/parameters = 22227/13/1305. CCDC 977704.

- D. Gatteschi, O. Kahn and R. D. Willet, Eds. *Magneto-Structural Correlations in Exchange-Coupled Systems*; D. Reidel: Dordrecht, 1985.
- (a) G. Aromí and E. K. Brechin, *Struct. Bonding*, 2006, **122**, 1; (b) R. Sessoli and A. K. Powell, *Coord. Chem. Rev.*, 2009, **253**, 2328.
- (a) A. K. Boudalis, Y. Sanakis, C. P. Raptopoulou and V. Psycharis, *Magnetism and Superconductivity in Low-Dimensional Systems: Utilization in Future Applications*, D. Stamopoulos (Ed.) Nova Science Publishers Inc., New York, 2008, pp. 1-77; (b) *Molecular Cluster Magnets*, R. E. P. Winpenny (Ed.), World Scientific Books, Singapore 2011.
- (a) A. G. Smith, P. A. Tasker and D. J. White, *Coord. Chem. Rev.*, 2003, **241**, 61; (b) C. J. Milios, S. Piligkos, E. K. Brechin, *Dalton Trans.*, 2008, 1809.
- A. J. Tasiopoulos and S. P. Perlepes, *Chem. Commun.*, 2003, 580.
- See for example: (a) G. L. Abbati, A. Cornia, A. C. Fabretti, A. Caneschi, and D. Gatteschi, *Inorg. Chem.*, 1998, **37**, 1430; (b) P.-P. Yang, *Z. Anorg. Allg. Chem.*, 2011, **637**, 567; (c) A. J. Tasiopoulos, T. A. O'Brien, K. A. Abboud and G. Christou, *Angew. Chem. Int. Ed.*, 2004, **43**, 345.
- R. P. John, K. Lee, M. S. Lah, *Chem. Commun.*, 2004, 2660.

- 8 W. H. Press, S. A. Teukolsky, W. T. Vetterling, B. P. Flannery, *Numerical Recipes in C: The Art of Scientific Computing*. Second Edition, Cambridge, Cambridge University Press, 1992.
- 9 N. Berg, T. Rajeshkumar, S. M. Taylor, E. K. Brechin, G. Rajaraman and L. F. Jones, *Chem. Eur. J.*, 2012, **18**, 5906.